Journal of Hazardous Materials 192 (2011) 593–598

Contents lists available at ScienceDirect

Journal of Hazardous Materials

journal homepage: www.elsevier.com/locate/jhazmat

Bioreduction of *para*-chloronitrobenzene in drinking water using a continuous stirred hydrogen-based hollow fiber membrane biofilm reactor

Siqing Xia [a,*], Haixiang Li [a], Zhiqiang Zhang [a], Yanhao Zhang [b], Xin Yang [a], Renyong Jia [a], Kang Xie [a], Xiaotian Xu [a]

[a] State Key Laboratory of Pollution Control and Resource Reuse, College of Environmental Science and Engineering, Tongji University, Shanghai 200092, PR China
[b] College of Municipal and Environmental Engineering, Shandong Jianzhu University, Jinan 250101, PR China

ARTICLE INFO

Article history:
Received 10 October 2010
Received in revised form 17 March 2011
Accepted 19 May 2011
Available online 12 June 2011

Keywords:
para-Chloronitrobenzene
Bioreduction
Hollow fiber membrane biofilm reactor
Hydrogen

ABSTRACT

para-Chloronitrobenzene (*p*-CNB) is particularly harmful and persistent in the environment and is one of the priority pollutants. A feasible degradation pathway for *p*-CNB is bioreduction under anaerobic conditions. Bioreduction of *p*-CNB using a hydrogen-based hollow fiber membrane biofilm reactor (HFMBfR) was investigated in the present study. The experiment results revealed that *p*-CNB was firstly reduced to *para*-chloraniline (*p*-CAN) as an intermediate and then reduced to aniline that involves nitro reduction and reductive dechlorination with H_2 as the electron donor. The HFMBfR had reduced *p*-CNB to a major extent with a maximum removal percentage of 99.3% at an influent *p*-CNB concentration of 2 mg/L and a hydraulic residence time of 4.8 h, which corresponded to a *p*-CNB flux of 0.058 g/m^2 d. The H_2 availability, *p*-CNB loading, and the presence of competing electron acceptors affected the *p*-CNB reduction. Flux analysis indicated that the reduction of *p*-CNB and *p*-CAN could consume fewer electrons than that of nitrate and sulfate. The HFMBfR had high average hydrogen utilization efficiencies at different steady states in this experiment, with a maximum efficiency at 98.2%.

1. Introduction

Chloronitrobenzenes are widely used as intermediates for chemical syntheses of drugs, herbicides, dyes, etc., and are known to be very toxic and resistant to microbial degradation due to the electron-withdrawing properties of nitro and chlorine groups [1,2]. The chloronitrobenzenes include three isomers, *ortho*-chloronitrobenzene (*o*-CNB), *meta*-chloronitrobenzene (*m*-CNB), and *para*-chloronitrobenzene (*p*-CNB). *p*-CNB is the most toxic formation of these isomers [3,4], and is one of the priority pollutants in the environment [5]. *p*-CNB is a hazardous material, which can cause methemoglobinemia in humans and animals [5,6], and is weakly mutagenic and carcinogenic [7,8]. To minimize the potential for adverse health effects, *p*-CNB concentration in drinking water supply source is regulated at 50 μg/L in China [9].

Thus far, several physicochemical methods such as ozonation, electrolysis, and catalytic reduction have been applied for the removal of *p*-CNB from waters [10–12]. These physicochemical methods are costly and often generate problematic residues. Biodegradation of *p*-CNB would be a desirable outcome under appropriate environmental conditions or in treatment technology. However, the electron-withdrawing properties of nitro and chlorine groups on the benzene molecule make *p*-CNB more difficult to degrade under aerobic conditions [1]. Thus, anaerobic microbial reduction is an important degradation pathway, because the microbial attack is easily carried out in the presence of electron donors. Several earlier studies have reported the transformations of chloronitrobenzenes involve nitro reduction and reductive dechlorination under anaerobic conditions [13,14], and the nitro reduction is the first stage during the transformation or mineralization of nitroaromatic compounds [13,15,16].

Several organic compounds can be used as electron donors for microbial reductive dechlorination of chlorinated organic compounds under anaerobic conditions [17–19], but the residual organic compounds are also problematic when used in drinking water treatment. For this reason, H_2 is considered as a clean, non-toxic, residual-free, and inexpensive inorganic electron donor to take the place of the extra organic compounds. H_2 was also found to be used for microbial reduction or reductive dechlorination of *N*-nitrosodimethylamine (NDMA), chlorophenols (CPs), trichloroethane (TCA), chloroform (CF), and trichloroethene (TCE) [20–23]. Nevertheless, biological reduction of *p*-CNB with H_2 as an electron donor was rarely discussed in the literature.

The hydrogen-based hollow fiber membrane biofilm reactor (HFMBfR), a new technology for bioreduction of oxidized contaminants in drinking water [24–29], delivers H_2 directly as the

* Corresponding author. Tel.: +86 21 65980440; fax: +86 21 65986313.
E-mail address: siqingxia@gmail.com (S. Xia).

0304-3894/$ – see front matter © 2011 Elsevier B.V. All rights reserved.
doi:10.1016/j.jhazmat.2011.05.060

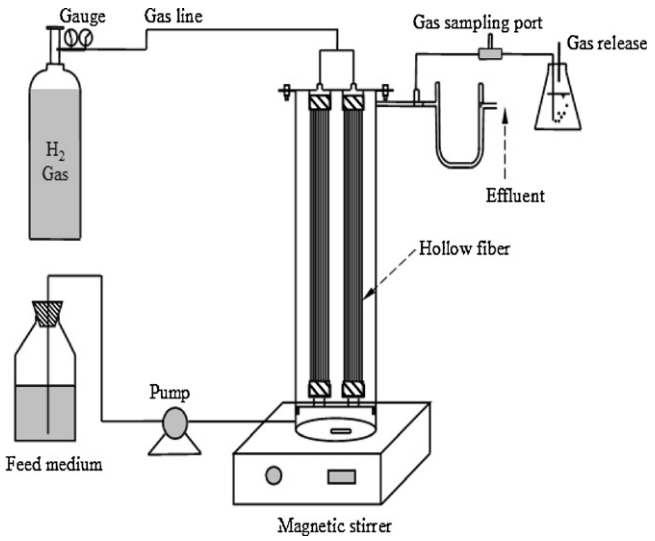

Fig. 1. Schematic of the bench-scale HFMBfR used to investigate *p*-CNB reduction.

electron donor by molecular diffusion through the micropores of a bubbleless gas-transfer membrane. The autotrophic bacteria (biofilm) lived on the outer surface of membrane oxidizes the H_2 to reduce one or several electron acceptors present in the water. Conventional drinking water treatment technology used in water treatment plant (WTP) cannot effectively remove the oxidized contaminants from water. Thus, the HFMBfR as an advanced treatment technology has been regarded as a potential cost-effective alternative for the treatment of these compounds. Furthermore, without addition of organic carbon source and water treatment agents makes effluent safer for human health. Therefore, this technology may provide an effective mechanism for removing *p*-CNB from drinking water by biodegradation. As a result, the toxicity of *p*-CNB will be largely reduced, and the biodegradability will also be enhanced in the following biological treatment process.

In the preliminary experiments, *p*-CNB bioreduction was evaluated to be feasible using hydrogenotrophic bacteria in the presence of H_2 in culture conditions. The major objectives of the present study were to investigate autohydrogenotrophic bioreduction of *p*-CNB using a novel set-up of continuous stirred polyvinyl chloride (PVC) hollow fiber membrane biofilm reactor, including (1) *p*-CNB bioreduction in the HFMBfR, (2) transformations of *p*-CNB, (3) analysis of competition between different electron acceptors, and (4) hydrogen utilization.

2. Materials and methods

2.1. Hollow fiber membrane biofilm reactor

The experimental set-up of the continuous stirring HFMBfR used in this study is shown in Fig. 1. A transparent plastic cylinder was used as a hollow fiber membrane reactor, in which two modules were directly submerged in the bulk fluid. The system behaved as a completely mixed biofilm reactor because of stirring power generated by a magnetic stirrer set in the bottom of the reactor. It is a major difference from the previously reported HFMBfRs that mix liquid by internal refluxing [24–26]. Pure H_2 was supplied to the inside hollow fibers from an H_2 gas tank. The hydrophobic hollow fibers were made of a novel material of polyvinyl chloride (PVC), manufactured by Litree Company (Suzhou, China). The physical characteristics of the HFMBfR are listed in Table 1. There are some advantages compared to the previously reported HFMBfRs [24–26]. PVC, as a synthetic material, was extensively used in drinking water supply systems in China. Compared to the composite material, PVC hollow fiber was economic in manufacturing and engineering applications. Earlier study of our group had shown that microorganisms attached to the outer surface of the membranes more easily to form a biofilm in the HFMBfR [28]. The modules were easily disassembled from the reactor for rinsing when the membranes were polluted or collecting biofilm samples from membranes.

Table 1
The physical characteristics of the HFMBfR system.

	Units	Value
Reactor height	cm	22
Reactor inner diameter	cm	7
Reactor available volume	cm^3	625
Feed rate	mL/min	2
Retention time	h	5.2
Number of hollow fibers		132
Membrane active length	cm	18
Membrane pore size	μm	0.01
Membrane inner diameter	cm	0.085
Membrane outside diameter	cm	0.15
Membrane surface area	cm^2	990

2.2. Inoculation, start-up, and experimental conditions

The HFMBfR was inoculated with a seeding bacteria source from another lab-scale hollow fiber membrane biofilm reactor, which treated nitrate contaminated drinking water over 100 days and had two modules when the inoculum was obtained [28]. Biofilm samples were collected from modules and mixed together. This mixture was added to a sterile glycerol solution. For inoculating the HFMBfR, the biomass from the mixture was centrifuged for 10 min at 7000 g and resuspended in sterile water. Then, a 50 mL washed biomass suspension was added into the HFMBfR system.

Start-up of the continuous stirred HFMBfR began when H_2 was supplied to the membrane under the pressure of 0.04 MPa. To establish biofilm on the membrane surface, the reactor was operated intermittently before continuous running. An influent with nitrate concentration at 5 mg NO_3^--N/L was fed continuously at 1.2 mL/min into HFMBfR for 20 h, and then the influent and H_2 supplies were closed for 4 h in one day. Repeat the above operations until the biofilm formed. We found some festucine flocculent biomass generated on the outer surface of the membranes around 10 days. After that, the feed rate of influent was set to 2.0 mL/min for continuous running with an influent nitrate of 10 mg NO_3^--N/L and sulfate of 55 mg SO_4^{2-}/L. The nitrate concentration in effluent reached a steady state after around 30 days, and then *p*-CNB was added to the influent of HFMBfR. Then, the bioreduction of *p*-CNB in the continuous stirred HFMBfR was investigated over 140 days with varied influent concentrations and hydrogen pressure.

Nitrate and sulfate were added to influent for more realistic simulation of drinking water in the experiment, because nitrate and sulfate are common oxidized contaminants in surface water or groundwater. Therefore, the addition of nitrate and sulfate was used for evaluating their effects on the *p*-CNB reduction and the competition for electron donors between these different electron acceptors.

2.3. Synthetic culture medium

The components of HFMBfR influent were (in g/L): KH_2PO_4 (0.128), Na_2HPO_4 (0.434), $MgSO_4{\cdot}7H_2O$ (0.2), $CaCl_2{\cdot}2H_2O$ (0.001), $FeSO_4{\cdot}7H_2O$ (0.001), $NaHCO_3$ (0.252), $NaNO_3$ (0.03), and 1 mL of trace mineral solution, respectively. The trace mineral solution (in mg/L) consisted of $ZnSO_4{\cdot}7H_2O$ (100), $MnCl_2{\cdot}4H_2O$ (30), H_3BO_3 (300), $CoCl_2{\cdot}6H_2O$ (200), $CuCl_2{\cdot}2H_2O$ (10), $NiCl_2{\cdot}6H_2O$ (10), $Na_2MoO_4{\cdot}2H_2O$ (30), and Na_2SeO_3 (30). The culture medium was

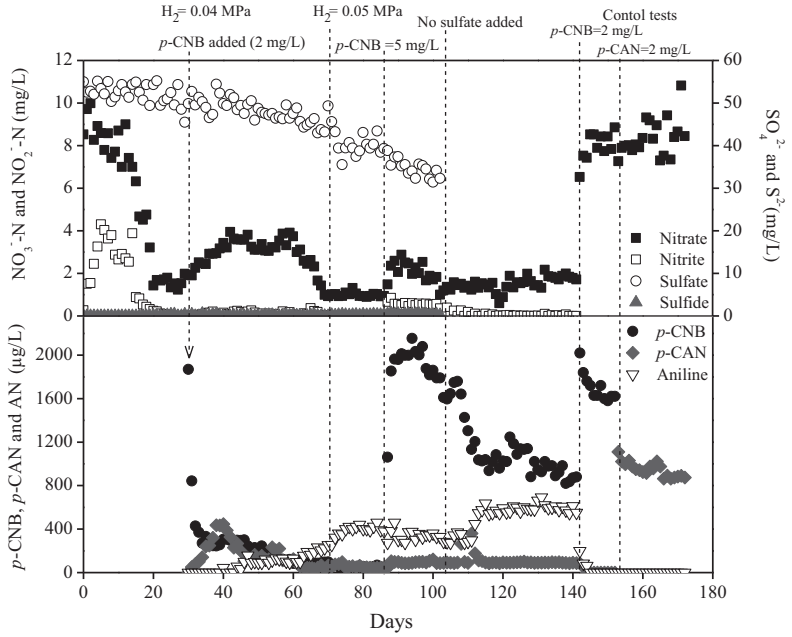

Fig. 2. Concentrations of *p*-CNB, *p*-CAN, aniline, nitrate, nitrite, sulfate, and sulfide in the effluent of the HFMBfR.

prepared in a 10.0 L (available volume) brown glass bottle under the purge by nitrogen gas to eliminate dissolved oxygen. $NaNO_3$ and $NaHCO_3$ were used as an inorganic nitrogen and carbon source for the growth of autotrophic microorganisms, respectively. Phosphate buffer ($KH_2PO_4 + Na_2HPO_4$) was used to keep initial pH of the influent around 7.5 and to prevent pH sharp rise during the reduction process.

2.4. Sampling and analysis

All the fluid samples collected from the reactor on a daily basis were immediately filtered through a 0.22 μm membrane filter (Anpel Co., Shanghai) and analyzed within 2 days. The concentrations of nitrate, nitrite, sulfate, dissolved sulfide and total organic carbon (TOC) were analyzed according to the standard methods of Chinese National Environmental Protection Administration [30]. Analyses for nitrate, nitrite, and sulfate were carried out by ion chromatography (ICS-1000, Dionex) using an AS-19 column (4 × 250 mm, Dionex). Dissolved sulfide was measured using a colorimetric method based on methylene blue formation. TOC analysis was performed with the Shimadzu TOC-VCPH analyzer. *p*-CNB, *p*-CAN and aniline were determined by HPLC (Agilent 1200, USA). Analysis parameters are listed as follows: column: Polaris C18, 5 μm, 4.6 × 250 mm; mobile phase: acetonitrile (ACN)/H_2O = 60/40 (v/v), flow rate: 1.0 mL/min; detector: UV at 254 nm, column temperature at 25 °C. The method detection limits for *p*-CNB, *p*-CAN and aniline were 16.8, 11.3 and 27.4 μg/L, respectively.

H_2 concentrations in effluent samples were determined by headspace-analysis method [31]. The gas sample in the headspace of the reactor was taken by inserting a gas-tight syringe through the rubber stopper on the gas-sampling port. The gas concentrations were measured by a GC 14-B quipped with a TCD detector (Shimadazu Co., Japan). The concentrations of H_2 in the liquid phase were calculated by headspace H_2 concentrations using Henry coefficients.

Organic compounds, such as *p*-CNB, *p*-CAN, aniline, and ACN are HPLC grade and obtained from Sigma. All other chemicals employed are of analytical grade and obtained from Sinopharm Chemical Reagent Co., Shanghai.

3. Results and discussion

3.1. Bioreduction of p-CNB in the HFMBfR

After 10 days of intermittently running, the bioreduction of nitrate, sulfate and *p*-CNB in the continuous stirred HFMBfR was investigated continuously over 170 days (Fig. 2). In the first few days of operation, the influent concentrations were only 10 mg NO_3^--N/L and 55 mg SO_4^{2-}/L with applied H_2 pressure at 0.04 MPa. The biofilm was built on the fibers gradually, and nitrate was partially converted to nitrite. Nitrate concentration in effluent gradually decreased within 20 days. Sulfate reduction began within 5 days of operation resulted in by-product sulfide.

On day 30, *p*-CNB was added to the influent with concentration of 2000 μg/L, and the H_2 pressure was also kept on 0.04 MPa. *p*-CNB was reduced immediately within 3 days of its addition, indicated by 100 μg/L of *p*-CAN on day 33 (Fig. 2). The concentration of *p*-CNB in effluent gradually decreased within 40 days. *p*-CAN reached at its highest concentration on day 40 (446 μg/L), and then it decreased continually. *p*-CAN began to be reduced to aniline (dechlorination) on day 44, or 14 days after *p*-CNB addition. A faster reduction of *p*-CNB to aniline (97 μg/L of *p*-CNB, or a 4.9% residual) was evident by day 70, corresponding to 253 μg/L of effluent aniline concentration.

The H_2 pressure was changed to 0.05 MPa to enhance the *p*-CNB reduction on day 71, which increased continually up to day 86 by achieving a maximum aniline concentration of 460 μg/L. The total quantity of *p*-CNB reduction was greatly enhanced with increasing the influent *p*-CNB concentration to 5000 μg/L (on day 87), but the removal percentage of *p*-CNB declined to 63.1%. The *p*-CNB reduction increased gradually without sulfate addition in influent from day108 (Fig. 2). From day 135 to day 141, the fifth steady state was achieved with a *p*-CNB concentration of 886 ± 54 μg/L and an aniline concentration of 582 ± 27 μg/L.

In order to determine whether *p*-CNB was bioreduced in the absence of H_2 in the HFMBfR, we stopped H_2 gas supply to the reactor from day 142 to day 172 (Fig. 2). The feed rate of influent was 2.0 mL/min. Influent *p*-CNB, *p*-CAN, and nitrate concentrations were 2000 μg/L, 1000 μg/L (from day 153) and 10 mg/L, respectively. The nitrate concentration in effluent during the period of control tests changed slightly (nearly 8 mg/L). The *p*-CNB and *p*-CAN

degradation rates without H_2 supplying were obviously lower than that with H_2 supplying. Therefore, the results obtained in the control tests suggest that *p*-CNB bioreduction occurred in the presence of H_2 as an effective electron donor in HFMBfR.

Table 2 presents the results of four steady states of the experiment. The key conclusion from the steady states is that H_2 pressure, *p*-CNB loading, and sulfate concentration controlled the *p*-CNB reduction. A *p*-CNB flux of 0.058 g/m^2 of biofilm surface area/day gave an effluent aniline concentration of 406 μg/L and 99.3% of *p*-CNB removal percentage when the H_2 pressure was turned to 0.05 MPa. Increasing the *p*-CNB concentration from 2000 μg/L to 5000 μg/L in influent generated a higher *p*-CNB flux of 0.097 g/m^2 d for the same H_2 pressure, but declined the *p*-CNB removal percentage to 63.1%. Absence of sulfate in influent allowed a higher *p*-CNB flux of 0.117 g/m^2 d and *p*-CNB removal percentage of 81.9% than 55 mg/L of sulfate in influent for the same H_2 pressure and *p*-CNB influent concentration. Sulfate reduction to sulfide consumes 8e$^-$ eq/mol, which means that the concentration of sulfate was a high H_2 consumer in the reactions. In other words, sulfate as electron acceptor would compete for H_2 availability. Thus, the absence of sulfate was expected to positively enhance the bioreduction of *p*-CNB to aniline. TOC tests showed that effluent TOC concentration had a little increase compared to influent TOC concentration, which may be attributed to the generation of soluble microbial products (SMP) during the growth of microorganisms [24,32].

3.2. Transformations of p-CNB

Bioreduction of *p*-CNB occurred in the HFMBfR with H_2 as the electron donor when *p*-CNB was added to the influent (Fig. 2). The intermediate detected in the experiment indicates that the reduction of the nitro group was the first step in the transformations of *p*-CNB, resulting in the formation of corresponding *p*-CAN. The *p*-CAN further transformed via *para* dechlorination pathway to yield product of aniline (Fig. 3). The Gibbs free energy (−122.7 kJ/mol) and redox potential (226 mV) for the reductive dechlorination of *p*-CAN with H_2 as the electron donor could be a good indicator of the reaction mechanism [33]. Furthermore, the *para* position of chlorine atom on the aromatic ring makes the bonds more labile for microbial attack [34,35]. Thus, the formed aniline confirmed the reductive dechlorination of *p*-CAN. However, the aniline concentration accumulation in the liquid was less than the amount of *p*-CNB and *p*-CAN reductions. Considering the presence of autotrophic bacteria in the reactor under anaerobic conditions, one possible reason for aniline disappearance was its instability during the sampling and analysis in an air and light circumstance [36]. Although aniline as final product was non-biodegradable in the system, the biological reduction process reduced the toxicity of *p*-CNB and enhanced the biodegradability of the effluent.

3.3. Flux analysis

Nitrate and sulfate as conventional pollutants in drinking water were added to influent of HFMBfR to evaluate the competition of H_2 availability among *p*-CNB, nitrate, and sulfate. Table 3 shows the electron-equivalent fluxes of electron acceptors and the percentage distributions of each flux at the different steady states. Nitrate reduction was the biggest consumer of electrons (60.0–93.6%), and the second biggest was sulfate reduction (21.3–36.7%). Reduction of *p*-CNB to *p*-CAN was a small percentage of electron fluxes (1.7–4.9%). The smallest percentage was reductive dechlorination of *p*-CAN to aniline (0.5–1.5%). These mean that the total demand for H_2 was largely controlled by nitrate and sulfate reduction. The electron-equivalent fluxes of *p*-CNB and *p*-CAN responded positively to higher H_2 availability (day 80–86), higher *p*-CNB loading (day 98–102) and lower sulfate loading (day 135–141). The

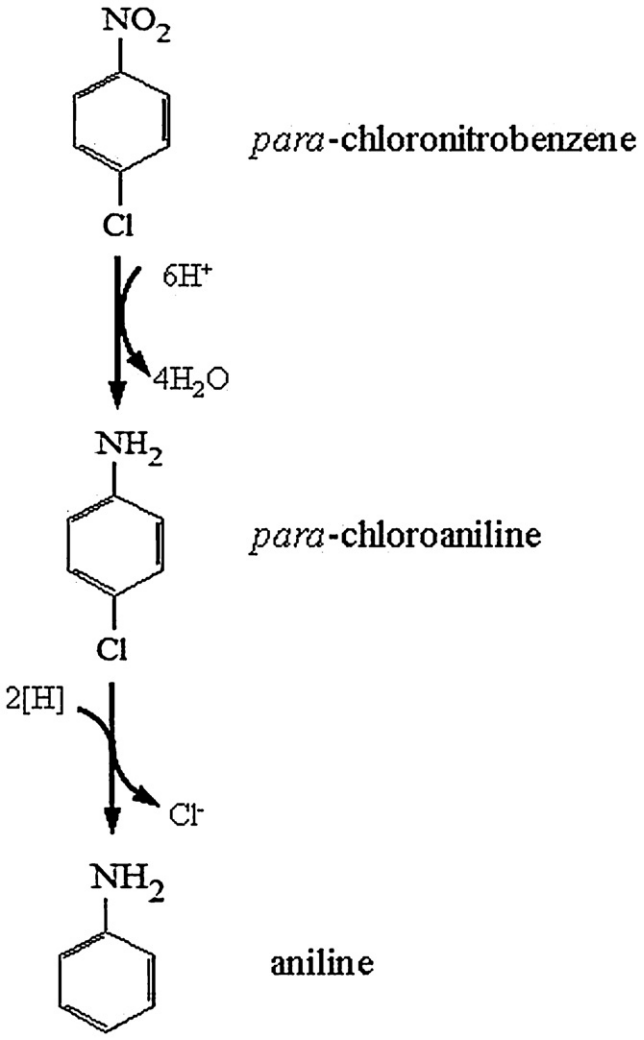

Fig. 3. The proposed transformation pathway of *p*-CNB in HFMBfR.

results present here demonstrate that *p*-CNB was bioreduced in the HFMBfR in which the electron-equivalent fluxes from H_2 oxidation were dominated by nitrate and sulfate reductions (>95%).

3.4. Hydrogen utilization

In this study, hydrogen consumption was mainly attributed to *p*-CNB, nitrate and sulfate reductions. We analyzed the sum of hydrogen utilization rates during *p*-CNB, nitrate and sulfate reductions by the biofilm (R_{HB}, mg H_2/cm^3 d), the hydrogen fluxes transferred from the membrane into the biofilm (J_{HT}, mg H_2/cm^2 d), and the hydrogen utilization efficiencies (%) for *p*-CNB, nitrate and sulfate reductions under the fundamental assumptions. The assumptions are (1) the substrate utilized by suspended biomass is insignificant, and (2) biomass is not included in the mass balances because of low biomass yield [37].

The average hydrogen utilization rates at these steady states were between 0.015 and 0.024 mg H_2/cm^3 d, which corresponded to hydrogen fluxes from 0.010 to 0.014 mg H_2/cm^2 d (Fig. 4). Lee and Rittmann [37] has reported that hydrogen fluxes of autohydrogenotrophic denitrification were from 0.012 to 0.014 mg H_2/cm^2 d. Both increasing the *p*-CNB loading and the supplied H_2 pressure increased the hydrogen utilization rates and hydrogen fluxes. The effluent hydrogen concentration decreased as *p*-CNB loading increasing and sulfate presence in influent (data

Table 2
Summary of the steady state results for the HFMBfR.

Parameters	Steady state periods (days)			
	65–70	80–86	98–102	135–141
H_2 pressure (MPa)	0.04	0.05	0.05	0.05
Average influent *p*-CNB (μg/L)	1980	2055	4950	4890
Average influent TOC (mg C/L)	–	2.1	–	3.3
Average effluent *p*-CNB (μg/L)	90 ± 23	55 ± 16	1827 ± 139	886 ± 54
Average effluent *p*-CAN (μg/L)	50 ± 15	45 ± 10	99 ± 14	90 ± 18
Average effluent aniline (μg/L)	211 ± 32	406 ± 27	342 ± 13	582 ± 27
Average effluent nitrate (mg NO_3^--N/L)	1.66 ± 0.69	0.96 ± 0.06	1.62 ± 0.36	1.82 ± 0.10
Average effluent sulfate (mg SO_4^{2-}/L)	45 ± 2	41 ± 2	33 ± 1	–
Average effluent TOC (mg C/L)	–	2.4 ± 0.1	–	3.9 ± 0.3
Average removal of *p*-CNB	95.4%	99.3%	63.1%	81.9%
p-CNB flux (g *p*-CNB/m^2 d)	0.055	0.058	0.097	0.117
Nitrate flux (g NO_3^--N/m^2 d)	0.243	0.263	0.244	0.238
Sulfate flux (g SO_4^{2-}/m^2 d)	0.291	0.407	0.640	–

Table 3
Electron-equivalent fluxes for *p*-CNB, *p*-CAN, nitrate, and sulfate at steady states.

Periods (days)	Electron-equivalent flux				Sum up the fluxes	Distribution of Electron-equivalent fluxes			
	p-CNB[a] eq/m^2 d	*p*-CAN[b]	Nitrate[c]	Sulfate[d]	eq/m^2 d	*p*-CNB %	*p*-CAN	Nitrate	Sulfate
65–70	0.0021	0.0007	0.0868	0.0243	0.1139	1.9	0.6	76.2	21.3
80–86	0.0022	0.0007	0.0939	0.0339	0.1307	1.7	0.5	71.8	26.0
98–102	0.0037	0.0011	0.0871	0.0533	0.1452	2.5	0.8	60.0	36.7
135–141	0.0044	0.0014	0.0850	–	0.0908	4.9	1.5	93.6	–

[a] Calculated by $J_{e^-p\text{-CNB}} = \frac{\text{Influent flow rate}\,(Q)\times\text{removed }p\text{-CNB}\,(\Delta S)}{\text{Total bofilm surface}\,(aV)\times EW_{p\text{-CNB}}}$, where Q is in m^3/d, ΔS is in g *p*-CNB/m^3, aV is in m^2, $EW_{p\text{-CNB}}$ is 26.3 in g *p*-CNB/e^- equivalent for reduction of *p*-CNB to *p*-CAN.

[b] Calculated by $J_{e^-p\text{-CAN}} = \frac{\text{Influent flow rate}\,(Q)\times\text{removed }p\text{-CAN}\,(\Delta S)}{\text{Total bofilm surface}\,(aV)\times EW_{p\text{-CAN}}}$, where Q is in m^3/d, ΔS is in g *p*-CAN/m^3, aV is in m^2, $EW_{p\text{-CAN}}$ is 63.8 in g *p*-CAN/e^- equivalent for reduction of *p*-CAN to aniline.

[c] Calculated by $J_{e^-NO_3^--N} = \frac{\text{Influent flow rate}\,(Q)\times\text{removed }NO_3^--N\,(\Delta S)}{\text{Total bofilm surface}\,(aV)\times EW_{NO_3^--N}}$, where Q is in m^3/d, ΔS is in g NO_3^--N/m^3, aV is in m^2, $EW_{Nitrate}$ is 2.8 in g NO_3^--N/e^- equivalent for reduction of nitrate to nitrogen gas.

[d] Calculated by $J_{e^-SO_4^{2-}} = \frac{\text{Influent flow rate}\,(Q)\times\text{removed }SO_4^{2-}\,(\Delta S)}{\text{Total bofilm surface}\,(aV)\times EW_{SO_4^{2-}}}$, where Q is in m^3/d, ΔS is in g SO_4^{2-}/m^3, aV is in m^2, $EW_{Sulfate}$ is 12 in g SO_4^{2-}/e^- equivalent for reduction of sulfate to sulfide.

not shown). With the reactor running, the average hydrogen utilization efficiency changed gradually at these five steady states, for seen 89.4%, 95.3%, 95.3%, 98.2%, and 96.7%, respectively. The results are close to Xia et al. [28] and Lee and Rittmann [37] of nearly 100% hydrogen utilization efficiencies in their membrane biofilm reactors. This innovative gas-transfer technology achieved high hydrogen utilization efficiency by dissolving H_2 directly into the water without bubble formation that contributes to homogeneous diffusion. High hydrogen utilization efficiency indicates the advantage of bitty-residual of H_2, which promotes the application of this technology in treatment of oxidized contaminants.

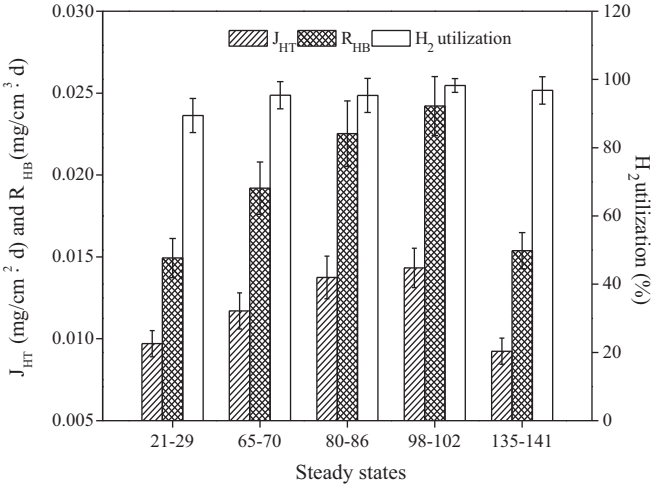

Fig. 4. Average hydrogen utilization rates, hydrogen fluxes and hydrogen utilization efficiencies at different steady states.

4. Conclusions

The performance of HFMBfR demonstrated that *p*-CNB can be bioreduced to *para*-chloroaniline (*p*-CAN) as intermediate by hydrogenotrophic bacteria with H_2 as the electron donor, and then to aniline by dechlorinating so as to reduce the toxicity of *p*-CNB and enhance the biodegradability of drinking water contaminated with *p*-CNB. A good bioreduction efficiency could be achieved by the continuous stirred HFMBfR using PVC membranes, with a maximum *p*-CNB reduction flux of 0.117 g/m^2 d. *p*-CNB reduction responded to *p*-CNB loading, H_2 pressure, and the presence of electron competitors. Analysis of electron-equivalent fluxes showed that the reductions of *p*-CNB and *p*-CAN could consume fewer electrons than that of nitrate and sulfate. The rate and efficiency of hydrogen utilization by biofilm were achieved as high as 0.024 mg H_2/cm^3 d and 98.2%, respectively. Bioreduction using the hollow fiber membrane biofilm reactor is a promising technology for treatment of *p*-CNB in drinking water.

Acknowledgements

We acknowledge the support provided by National Natural Science Foundation of China (50978190), National High Technology Research and Development Program of China (2009AA062902),

and Water Pollution Control in Water System of Small Towns (2009ZX07317-008-5).

References

[1] H.S. Park, S.J. Lim, Y.K. Chang, A.G. Livingston, H.S. Kim, Degradation of chloronitrobenzenes by a co-culture of *Pseudomonas* putida. and a *Rhodococcus* sp, Appl. Environ. Microbiol. 65 (1999) 1083–1091.

[2] J.F. Wu, C.Y. Jiang, B.J. Wang, Y.F. Ma, Z.P. Liu, S.J. Liu, Novel partial reductive pathway for 4-chloronitrobenzene and nitrobenzene degradation in *Comamonas* sp. strain CNB-1, Appl. Environ. Microbiol. 72 (2006) 1759–1765.

[3] S.G. Davydova, A comparison of the properties of nitrochlorobenzene isomers for the determination of their permissible concentrations in water bodies, Hyg. Sanit. 32 (1967) 161–166.

[4] T. Watanabe, N. Ishihara, M. Ikeda, Toxicity of and biological monitoring for 1,3-diamino-2,4,6-trinitrobenzene and other nitro-amino derivatives of benzene and chlorobenzene, Int. Arch. Occup. Environ. Health 37 (1976) 157–168.

[5] European Economic Community, Communication from the commission to the council on dangerous substances which might be included in list I of council directive 76/464/EEC, Brussels, Belgium, 1982.

[6] A.L. Linch, Biological monitoring for industrial exposure to cyanogenic aromatic nitro and amino compounds, Am. Ind. Hyg. Assoc. J. 35 (1974) 426–432.

[7] M. Shimizu, T. Yasui, N. Matsumoto, Structural specificity of aromatic compounds with special reference to mutagenic activity in Salmonella typhimurium–a series of chloro- or fluoro-nitrobenzene derivatives, Mutat. Res. 116 (1983) 217–238.

[8] E.K. Weisburger, F. Russfield, J. Homburger, J.H. Weisburger, E. Boger, C.G. Van Dongen, K.C. Chu, Testing of twenty-one environmental aromatic amines or derivatives for long-term toxicity or carcinogenicity, Environ. Pathol. Toxicol. 2 (1978) 325–356.

[9] Chinese Ministry of Health, Sanitary standards for drinking water quality (GB/T 5750-2001), 2001.

[10] J.M. Shen, Z.L. Chen, Z.Z. Xu, X.Y. Li, B.B. Xu, F. Qi, K Kinetics and mechanism of degradation of *p*-chloronitrobenzene in water by ozonation, J. Hazard. Mater. 152 (2008) 1325–1331.

[11] Y.J. Liu, Aqueous *p*-chloronitrobenzene decomposition induced by contact glow discharge electrolysis, J. Hazard. Mater. 166 (2009) 1495–1499.

[12] T.Y. Zhang, L.Y. You, Y.L. Zhang, Photocatalytic reduction of *p*-chloronitrobenzene on illuminated nano-titanium dioxide particles, Dyes Pigments 68 (2006) 95–100.

[13] C.G. Heijman, C. Hollinger, M.A. Claus, R.P. Schwarzenbach, J. Zeyer, Abiotic reduction of 4-chloronitrobenzene to 4-chloroaniline in a dissimilatory iron-reducing enrichment culture, Appl. Environ. Microbiol. 59 (1993) 4350–4353.

[14] S. Susarla, S. Masunaga, Y. Yonezawa, Transformations of chloronitrobenzenes in anaerobic sediment, Chemosphere 32 (1996) 967–977.

[15] D.L. Macalady, P.G. Tratnyek, T.J. Grundl, Abiotic reduction reactions of anthropogenie organic chemicals in anaerobic systems: a critical review, J. Contam. Hydrol. 1 (1986) 1–28.

[16] L.E. Hallas, M. Alexander, Microbial transformation of nitroaromatic compounds in sewage effluent, Appl. Environ. Microbiol. 45 (1983) 1234–1241.

[17] R.S. Booker, S.G. Pavlostathis, Microbial reductive dechlorination of hexachloro-1,3-butadiene in a methanogenic enrichment culture, Water Res. 34 (2000) 4437–4445.

[18] P. Bennett, D. Gandhi, S. Warner, J. Bussey, In situ reductive dechlorination of chlorinated ethenes in high nitrate groundwater, J. Hazard. Mater. 149 (2007) 568–573.

[19] I. Panagiotakis, D. Mamais, M. Pantazidous, M. Mameri, M. Parapoli, E. Hatziloukas, V. Tandoi, Dechlorinating ability of TCE-fed microcosms with different electron donors, J. Hazard. Mater. 149 (2007) 582–589.

[20] C.C. Chang, S.K. Tseng, C.C. Chang, C.M. Ho, Reductive dechlorination of 2-chlorophenol in a hydrogenotrophic, gas-permeable, silicone membrane bioreactor, Biores. Technol. 90 (2003) 323–328.

[21] J. Chung, B.E. Rittmann, Bio-reductive dechlorination of 1,1,1-trichloroethane and chloroform using a hydrogen-based emmbrane biofilm reactor, Biotechnol. Bioeng. 97 (2007) 52–60.

[22] J. Chung, C.H. Ahn, Z. Chen, B.E. Rittmann, Bio-reduction of *N*-nitrosodimethylamine (NDMA) using a hydrogen-based membrane biofilm reactor, Chemosphere 70 (2007) 516–520.

[23] J. Chung, B.R. Krajmalnik, B.E. Rittamnn, Bio-reduction of trichloroethene using a hydrogen-based membrane biofilm reactor, Environ. Sci. Technol. 42 (2008) 477–483.

[24] S.J. Ergas, A.F. Reuss, Hydrogenotrophic denitrification of drinking water using a hollow fiber membrane bioreactor, J. Water Supply Res. T. 50 (2001) 161–171.

[25] R. Nerenberg, B.E. Rittmann, Hydrogen-based hollow-fiber membrane biofilm reactor for reduction of perchlorate and other oxidized contaminants, Water Sci. Technol.: Water Supply 49 (2004) 223–230.

[26] B.E. Rittmann, R. Nerenberg, K.C. Lee, I. Najm, T.E. Gillogly, G.E. Lehman, S.S. Adham, Hydrogen-based hollow-fiber membrane biofilm reactor (MBfR) for removing oxidized contaminants, Water Sci. Technol.: Water Supply 4 (2004) 127–133.

[27] R. Nerenberg, B.E. Rittmann, I. Najm, Perchlorate reduction in a hydrogen-based membrane biofilm reactor, J. Am. Water Works Assoc. 94 (2002) 103–114.

[28] S.Q. Xia, Y.H. Zhang, F.H. Zhong, A continuous stirred hydrogen-based polyvinyl chloride membrane biofilm reactor for the treatment of nitrate contaminated drinking water, Biores. Technol. 100 (2009) 6223–6228.

[29] Y.H. Zhang, F.H. Zhong, S.Q. Xia, X.J. Wang, J.X. Li, Autohydrogenotrophic denitrification of drinking water using a polyvinyl chloride hollow fiber membrane biofilm reactor, J. Hazard. Mater. 170 (2009) 203–209.

[30] Chinese National Environmental Protection Administration, Water and wastewater monitoring methods, fourth ed., Chinese environmental science publishing house, Beijing, China, 2002.

[31] J.E. Schmidt, B.K. Ahring, Effects of hydrogen and formate on the degradation of propionate and butyrate in thermophilic granules from an up flow anaerobic sludge blanket reactor, Appl. Environ. Microbiol. 59 (1993) 2546–2551.

[32] K.C. Lee, B.E. Rittmann, A novel hollow fiber membrane biofilm reactor for autohydrogenotrophic denitrification of drinking water, Water Sci. Technol. 41 (2000) 219–226.

[33] S. Susarla, S. Masunaga, Y. Yonezawa, Redox potential as a parameter to predict the reductive dechlorination pathway of chloroanilines in anaerobic environments, Microb. Ecol. 33 (1997) 252–256.

[34] E.P. Kuhn, J.M. Suflita, Sequential reductive dehalogenation of chloroanilines by microorganisms from a methanogenic aquifer, Environ. Sci. Technol. 23 (1989) 848–852.

[35] S. Susarla, S. Masunaga, Y. Yonezawa, Reductive dechlorination pathways of chloro organics under anaerobic conditions, Water Sci. Technol. 34 (1996) 489–494.

[36] C.D. Lyons, S. Katz, R. Bartha, Mechanisms and pathways of aniline elimination from aquatic environments, Appl. Environ. Microbiol. 48 (1984) 491–496.

[37] K.C. Lee, B.E. Rittmann, Applying a novel autohydrogenotrophic hollow-fiber membrane biofilm reactor for denitrification of drinking water, Water Res. 36 (2002) 2040–2052.